Spectrochimica Acta Part A 81 (2011) 261–269

Contents lists available at ScienceDirect

Spectrochimica Acta Part A: Molecular and Biomolecular Spectroscopy

journal homepage: www.elsevier.com/locate/saa

Experimental and theoretical study on IR and NMR spectra of several tetrachlorinated diphenyl sulfides

Ruijuan Qu, Xuesheng Zhang, Qi Zhang, Xi Yang, Zunyao Wang*, Liansheng Wang

State Key Laboratory of Pollution Control and Resources Reuse, School of the Environment, Xianlin Campus, Nanjing University, Nanjing, Jiangsu 210046, PR China

ARTICLE INFO

Article history:
Received 4 December 2010
Received in revised form 13 June 2011
Accepted 14 June 2011

Keywords:
Tetrachlorinated diphenyl sulfides
B3LYP
IR
NMR chemical shifts

ABSTRACT

Tetrachlorinated diphenyl sulfides (TCDPSs) are environmentally interesting compounds. In this paper, both experimental and theoretical studies on IR and ^{1}H NMR as well as ^{13}C NMR chemical shifts of 4 synthesized TCDPSs have been carried out. The optimized geometries were obtained at the B3LYP/6-311G** level by using the Gaussian 03 program. Meanwhile, related spectral parameters were calculated. In addition, the experimental values were compared with the calculated ones. The results show that the scaled theoretical vibration frequencies are in good accordance with the observations, and computed chemical shifts are consistent with the experimental values.

1. Introduction

Polychlorinated diphenyl ethers (PCDEs), a group of halogenated aromatic compounds, are a subfamily of persistent organic pollutants (POPs). Due to their structural resemblance with PCDEs, polychlorinated diphenyl sulfides (PCDPSs) are environmentally interesting compounds [1]. Over the last 20 years, PCDPSs have been identified in various environmental samples: bleached pulp mill effluents, stack gas samples, fly ashes, pine needles, soil, sediments, tissues of aquatic biota [2]. PCDPSs in wastewater effluents may transfer to the atmosphere and result in emissions into acid rain and, consequently, accelerate the corrosion processes of steel [3]. The presence of PCDPSs in biota indicates that they are likely to bioaccumulate in lipids and they are able to be deposited in human tissues by biomagnification processes. Some PCDPSs which possess biological activity and phytotoxity are manufactured to be used as pesticides, such as 2,4,4′,5-tetrachlorodiphenyl sulfide [4]. Tetrachlorinated diphenyl sulfides (TCDPSs), a class of PCDPSs, have also been detected extensively in environment [5]. However, current researches on PCDPSs mainly focus on the configuration and reactions of the parent compound diphenyl sulfide (DPS) [6–9]. Meanwhile, the quantum chemical calculations for PCDPSs have so far been involved exclusively in the predictions of their thermodynamic properties [10]. Vibrational spectroscopy can be used to refine chemical structures, analyze the interactions between the various atoms of a compound, and predict the trends in the formation and breaking of chemical bonds. Moreover, nuclear magnetic resonance (NMR) spectroscopy is the most powerful method in analytical chemistry for the identifications of structural groups. Consequently, Experimental and theoretical study on the vibration spectra and NMR chemical shifts would be of significance in understanding their environmental behavior and potential environmental risk.

To obtain chemical shifts of molecules, density functional theory (DFT) is one of the most frequently used computational methods [11–13]. The nuclear shielding tensor is calculated for each atom via the GIAO (gauge-independant atomic orbital) approach. The details of the GIAO method have already been described elsewhere [14,15]. Absolute isotropic magnetic shielding constants were then converted into chemical shifts by referring to one of the standard compounds. In spite of the reliable methods for predicting ^{1}H chemical shifts [16,17], similar accuracy in the computation of ^{13}C chemical shifts has not been reached at least in many practical cases.

With regard to the theoretical spectra of compounds with complicated structures, especially in a non-planar geometry, the number of literatures is limited. Qiu et al. [18] calaulated IR and NMR parameters of 4,4′-dibromodiphenyl ether using the DFT method, and found that the calculated values agree well with the corresponding experimental ones.

In this paper, spectral properties (including IR, ^{1}H NMR and ^{13}C NMR) of 4 synthesized TCDPSs were thoroughly studied. The geometries of the title compounds were optimized at the B3LYP/6-311G** level with the Gaussian 03 program [19], and corresponding spectral parameters were also calculated with the same method. Additionally, comparisons of the experimental and the theoretical values were carried out.

---

* Corresponding author. Tel.: +86 25 89680358; fax: +86 25 89680358.
E-mail address: wangzun315cn@163.com (Z. Wang).

1386-1425/$ – see front matter © 2011 Elsevier B.V. All rights reserved.
doi:10.1016/j.saa.2011.06.008

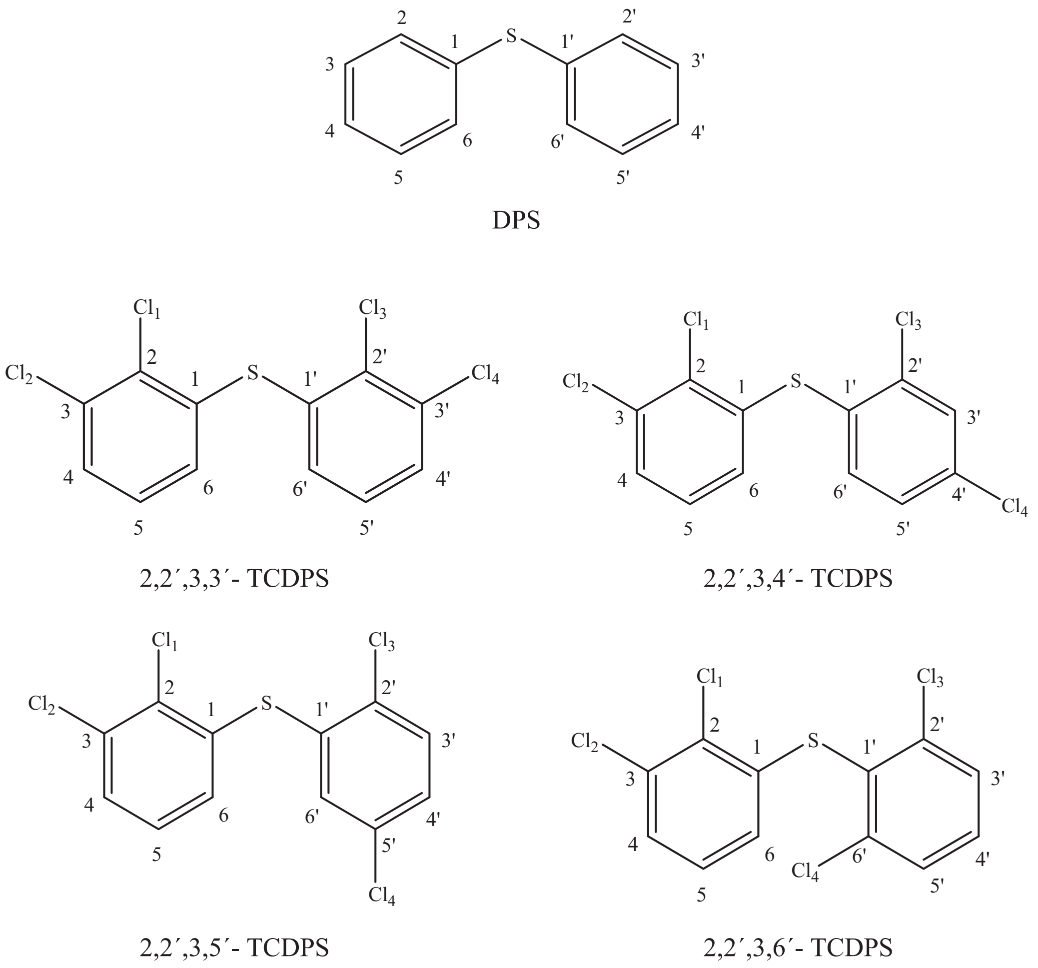

Fig. 1. The geometries and atomic numbering of the parent compound DPS and the four studied compounds.

2. Computational method

The 4 TCDPSs being studied are 2,2′,3,3′-TCDPS, 2,2′,3,4′-TCDPS, 2,2′,3,5′-TCDPS and 2,2′,3,6′-TCDPS. Molecular structures and atomic numbering of the parent compound DPS and the four title compounds are illustrated in Fig. 1. The structural geometries were optimized at the B3LYP/6-311G** level, and IR vibration frequencies as well as nuclear shielding tensors were calculated by using the Gaussian 03 program. There are no imaginary frequencies in the results of vibration analysis, which show that all the computations were converged on a true energy minimum. NMR chemical shifts have been calculated with the GIAO approach. Absolute isotropic magnetic shielding constants were transformed into chemical shifts ($\delta_i = \sigma_{\mathrm{TMS}} - \sigma_i$) by referring to one of the standard compounds, tetramethylsilane (TMS). By employing the animate vibration function of the Gaussview program [20], detailed assignments of the signals for each spectrum were made with a high degree of confidence.

Moreover, in order to compare the predictive ability of the DFT/GIAO approach for ^{13}C chemical shift calculations, the following empirical relationship was utilized to compute the spectroscopic data for the studied compounds.

$$\delta\mathrm{c}\,(\mathrm{ppm}) = 128.5 + \delta_0 + \delta\mathrm{o} + \delta\mathrm{o}' + \delta\mathrm{m} + \delta\mathrm{m}' + \delta\mathrm{p}$$

where δ_0 refers to the chemical shift of the atom (or group) which is directly connected to the carbon atom, δo, δo′, δm, δm′, and δp are contributions (increments) to chemical shifts that account for ortho (o), ortho′ (o′), meta (m), meta′ (m′), and para (p) substituents, respectively, and the free coefficient is the standard chemical shift of carbon atom.

3. Experiments

The studied solid TCDPSs were synthesized by ourselves. The general synthetic route is [21]:

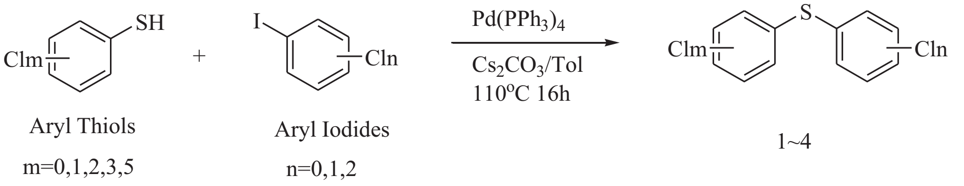

1~4

Table 1
The specific reactants used to synthesize the 4 title compounds and the yields [21].

Entry	Chloro thiophenols	Chloro iodobenzenes	Products	Yields (%)
1	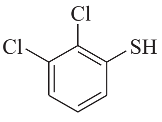	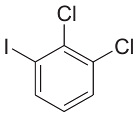	2,2′,3,3′-TCDPS	68
2	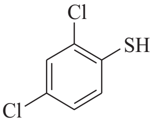	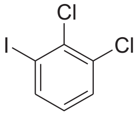	2,2′,3,4′-TCDPS	82
3	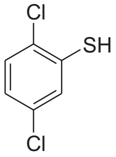	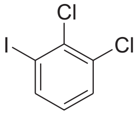	2,2′,3,5′-TCDPS	76
4	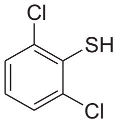	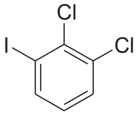	2,2′,3,6′-TCDPS	72

When it comes to the 4 title compounds, the specific reactants and yields are shown in Table 1. The following steps were adopted. 1 mmol of chloro thiophenol was dissolved in 10 ml of toluene. Next, 1 mmol of chloro iodobenzene and 2.5 mmol of cesium carbonate, together with 0.1 mmol of tetrakis (triphenylphosphine) palladium ($Pd(PPh_3)_4$, used as catalyst) were added into the mixture and the solution was heated to about 110 °C for 16 h under nitrogen. After cooling to room temperature, the solution was diluted with 100 ml of water and extracted 3 times with 20 ml of petroleum ether. The extract was dried with anhydrous magnesium sulfate, filtered and concentrated. The crude product obtained was further eluted with petroleum ether and then purified by silica gel column chromatography (300–400 mesh). Thus, the target products of high purity can be used for the determination of spectral properties. The IR spectra of the title compounds diluted in the KBr pellets were measured on a Nexus 470 FT-IR spectrophotometer in the range of 400–4000 cm^{-1} at room temperature. The ^1H NMR and ^{13}C NMR measurements were carried out using a Bruker Avance NMR spectrometer operating at 400 MHz at room temperature with TMS as an internal standard in $CDCl_3$.

4. Results and discussion

4.1. Optimized structures

Optimized bond lengths, bond angles and dihedral angles of the title compounds which are calculated at the B3LYP/6-311G** level are summarized in Table 2. It is found that the difference between the values of dihedral angles is the biggest. Since the experimental data are not available for the title compounds, the structural geometry of the parent compound DPS was optimized with the same method in order to test the reasonableness of the computational method. The optimized geometrical parameters of DPS can be obtained directly from Gaussian 03 output file. The X-ray diffraction values (obtained from literature [22]) are also listed in Table 3 for comparisons.

Clearly, the corresponding values calculated at the B3LYP/6-311G** level show excellent agreement with the experimental results, especially in the prediction of bond angles, despite the molecular geometry in the vapour phase may be different from that in the solid state. Consequently, the spectral parameters of the 4 title compounds may be accurately obtained with the same computational method.

Moreover, there exists an interesting relation between positions of Cl substituents and dihedral $C_{1'}$–S–C_1–C_6 and C_1–S–$C_{1'}$–$C_{6'}$ torsion angles. Similar to DPS, the sum of the two dihedral angles for the four TCDPSs is approximately equal to ±90°, indicating that the planes of the two benzene rings are almost perpendicular to each other. For 2,2′,3,3′-TCDPS, the values of the two dihedral angles $C_{1'}$–S–C_1–C_6 and C_1–S–$C_{1'}$–$C_{6'}$ are very close to that of DPS. For the other three title compounds, the dihedral angle values of $C_{1'}$–S–C_1–C_6 are all smaller than that of DPS, while the values of C_1–S–$C_{1'}$–$C_{6'}$ dihedral angle become larger compared with the corresponding value of DPS. For example, the dihedral angle C_1–S–$C_{1'}$–$C_{6'}$ of 2,2′,3,4′-TCDPS and 2,2′,3,5′-TCDPS is both −105.8°, and the value is 88.9° in 2,2′,3,6′-TCDPS. However, the sum of the two dihedral angles remains near ±90°.

4.2. Vibrational assignments

Calculated and experimental IR spectra of the 4 title compounds are shown in Fig. 2. It is obvious that the main absorption peaks of the calculated spectra basically coincide with those of the experimental spectra, indicating that the calculation results are reliable. Since anharmonicity effects in real system are neglected, the DFT method systematically overestimates the vibrational wave numbers [23]. Thus, generic frequency scale factors have to be applied in fitting the calculated values with experimental ones for B3LYP. In addition, increasing frequency overestimation of DFT in the high-frequency regions (>3000 cm^{-1}) was reported in several research papers [24,25]. Consequently, the frequencies of C–H stretching vibrations in this study were scaled down by multiplying a factor of 0.958 while other frequencies were scaled down by a factor of 0.9682 [26]. Furthermore, correlation analyses between scaled and experimental IR vibration frequencies were also carried out. The results are presented in Table 4. The squared correlation coefficients r^2 are all greater than 0.99, indicating that close relationships exist between theoretical frequencies and experimental values either for a single molecule or for all of them. In other words, IR vibration frequencies could be predicted by calculation with the Gaussian package. The band observed at about 3430 cm^{-1} in the experimen-

Table 2
Optimized parameters of the 4 title compounds.

Geometrical parameters	Name			
	2,2′,3,3′-TCDPS	2,2′,3,4′-TCDPS	2,2′,3,5′-TCDPS	2,2′,3,6′-TCDPS
Bond length (Å)				
rC_1-C_2	1.405	1.405	1.405	1.405
rC_2-C_3	1.402	1.398	1.398	1.398
rC_3-C_4	1.390	1.391	1.391	1.391
rC_4-C_5	1.391	1.389	1.389	1.389
rC_5-C_6	1.387	1.389	1.389	1.389
rC_1-C_6	1.399	1.396	1.396	1.396
rC_1-S	1.793	1.794	1.794	1.793
rC_2-Cl_1	1.745	1.747	1.747	1.747
rC_3-Cl_2	1.749	1.749	1.749	1.749
$rC_{2'}-Cl_3$	1.745	1.747	1.747	1.750
$rC_{3'(4',5',6')}-Cl_4$	1.749	1.753	1.755	1.749
Bond angle (°)				
$AC_6-C_1-C_2$	119.2	119.1	119.1	119.0
AC_6-C_1-S	120.7	123.3	123.3	123.5
AC_2-C_1-S	119.9	117.6	117.6	117.4
$AC_3-C_2-C_1$	119.5	119.9	119.8	119.9
$AC_4-C_3-C_2$	120.6	120.6	120.6	120.6
$AC_5-C_4-C_3$	119.7	119.3	119.3	119.3
$AC_6-C_5-C_4$	120.3	120.7	120.7	120.7
$AC_1-C_6-C_5$	120.6	120.5	120.5	120.5
AC_1-S-$C_{1'}$	101.9	103.1	102.9	102.6
$AC_{2'}-C_{1'}-C_{6'}$	119.2	118.0	118.7	117.0
$AS-C_{1'}-C_{6'}$	120.8	118.4	117.8	121.5
$AC_{2'}-C_{1'}-S$	119.8	123.3	123.2	121.3
Dihedral angle (°)				
$AC_{1'}-S-C_1-C_6$	−46.1	8.3	10.9	3.4
$AC_1-S-C_{1'}-C_{6'}$	−45.7	−105.8	−105.8	88.9

tal spectra is thought to be the characteristic absorption peak of water molecules. Take 2,2′,3,3′-TCDPS for example, the main calculated and experimental IR vibrational spectra are listed in Table 5. The vibrational assignments are briefly illustrated below.

The C–H stretching vibrations of aromatic structures often occur in the region of 3000–3100 cm^{-1} [27]. It is reported that the bands of the ring C–C stretching vibration generally appear at 1280–1380 cm^{-1}, 1430–1465 cm^{-1}, 1470–1540 cm^{-1}, 1575–1590 cm^{-1}, and 1590–1625 cm^{-1} in variable intensities [28]. Two weak bands observed at 3072 and 3046 cm^{-1} in experimental IR spectra are assigned as the aromatic C–H stretching vibration. The C=C aromatic semicircle stretching vibrations occurs at 1565 cm^{-1} and 1253 cm^{-1} in experimental IR spectra. The observation from the Gaussview program indicates that the very strong band around 1433 cm^{-1} results from the coupling between the C=C stretching vibrations and the C–H in-plane bending. That is the case of the strong band at 1397 cm^{-1}. The C–H in-plane bending vibrations usually occur in the region 1000–1300 cm^{-1} [29]. The infrared band at 1146 cm^{-1} with medium strong intensity and the medium band at 1194 cm^{-1} are assigned to C–H in-plane bending vibrations. The band appeared at 1086 cm^{-1} may be derived from the combination of the C–S symmetric stretching, C=C stretching vibrations and the C–H in-plane bending vibrations. The pure C–H out-of-plane vibration is not observed and is calculated at 764 cm^{-1}. The weak band at 706 cm^{-1} is assigned to C–H out-of-plane vibration being weakly coupled to ring deformation. It has been reported that the C–X group (X = Cl, Br, I) vibration often occurs in a wide range of 480–1290 cm^{-1} since its vibration is easily affected by the neighboring atoms or groups [30,31]. The peak observed at 1040 cm^{-1} is primarily assigned as the C–Cl stretching vibration, which is coupled with the trigonal ring breathing. Besides, C–Cl vibrations are often accompanied by C–S vibrations because the atomic weight of Cl is very close to that of S. The bands appeared at 782, 730 and 505 cm^{-1} are the results of the coupling of the C–S

Table 3
Calculated and experimental bond lengths, bond angels, dihedral angles of DPS.

Geometrical parameter	Cal.	Exp[a]	Diff.
Bond length (Å)			
rC_1-C_2	1.397	1.405	0.008
rC_2-C_3	1.394	1.399	0.005
rC_3-C_4	1.392	1.398	0.006
rC_4-C_5	1.395	1.401	0.006
rC_5-C_6	1.391	1.397	0.006
rC_1-C_6	1.399	1.405	0.006
rC_1-S	1.796	1.774	−0.022
Bond angle (°)			
$AC_6-C_1-C_2$	119.7	119.6	−0.1
AC_6-C_1-S	121.8	122.5	0.7
AC_2-C_1-S	118.3	117.9	−0.4
$AC_3-C_2-C_1$	120.0	120.0	0
$AC_4-C_3-C_2$	120.3	120.4	0.1
$AC_5-C_4-C_3$	119.7	119.6	−0.1
$AC_6-C_5-C_4$	120.4	120.4	0
$AC_1-C_6-C_5$	119.9	120.0	0.1
$AC_1-S-C_{1'}$	103.2	103.4	0.2
Dihedral angle (°)			
$AC_1{'}-S-C_1-C_6$	−50.1	−49.6	0.5
$AC_1-S-C_1{'}-C_6{'}$	−49.5	−49.6	−0.1

[a] The experimental data taken from Ref. [22].

Table 4
Correlation analysis of calculated and experimental IR vibrational frequencies.

Molecule	Correlation equations	r^2
2,2′,3,3′-TCDPS	$\lambda_{exp} = 24.053 + 0.990\lambda_{cal}$	1.000
2,2′,3,4′-TCDPS	$\lambda_{exp} = -16.468 + 1.016\lambda_{cal}$	0.999
2,2′,3,5′-TCDPS	$\lambda_{exp} = 8.882 + 1.002\lambda_{cal}$	1.000
2,2′,3,6′-TCDPS	$\lambda_{exp} = 15.565 + 1.003\lambda_{cal}$	1.000
Overall	$\lambda_{exp} = 9.920 + 1.002\lambda_{cal}$	0.999

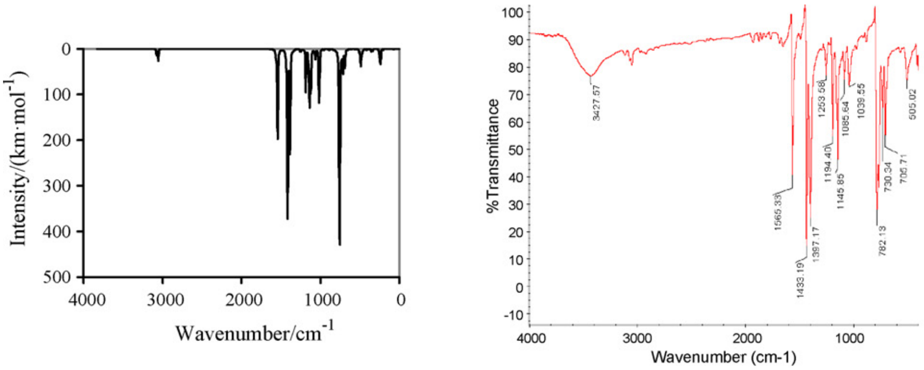

2,2′,3,3′- TCDPS (Cal.) 2,2′,3,3′- TCDPS (Exp.)

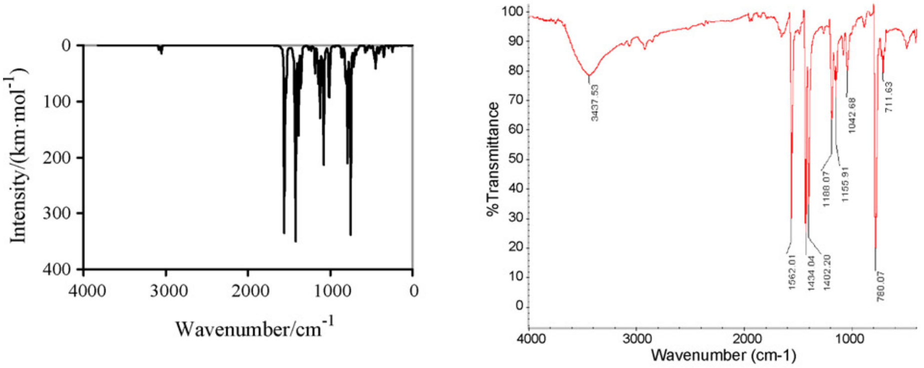

2,2′,3,4′- TCDPS (Cal.) 2,2′,3,4′- TCDPS (Exp.)

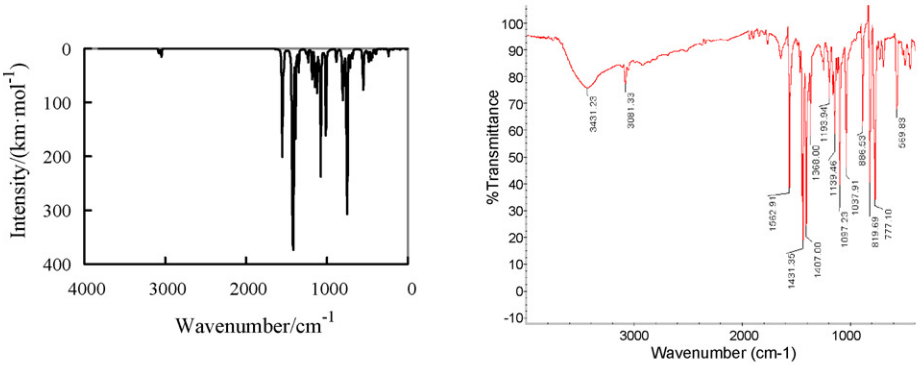

2,2′,3,5′- TCDPS (Cal.) 2,2′,3,5′- TCDPS (Exp.)

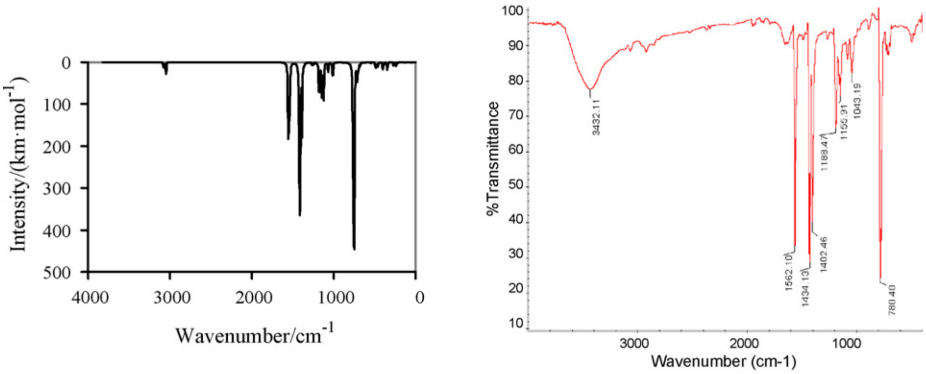

2,2′,3,6′- TCDPS (Cal.) 2,2′,3,6′- TCDPS (Exp.)

Fig. 2. Calculated and experimental IR spectra of the 4 title compounds.

Table 5
Comparison of the main calculated and experimental (IR) vibrational spectra of 2,2′,3,3′-TCDPS.

No.	Approximate assignments[a]	Experimental frequency[b]	Calculated		
			Frequency		Intensity
			Unscaled	Scaled[c]	
1	ν C–H	3072w	3216	3081	5.0
2	ν C–H	3046w	3184	3050	27.0
3	ν C=C	1565ms	1592	1541	198.2
4	ν C=C, β C–H	1433vs	1464	1417	371.2
5	ν C=C, β C–H	1397s	1432	1386	228.6
6	ν C=C	1253w	1320	1278	1.4
7	β C–H	1194m	1224	1185	94.8
8	β C–H	1146ms	1176	1139	128.5
9	ν_s C–S, ν C=C, β C–H	1086w	1104	1069	22.8
10	ν C–Cl, trigonal ring breathing	1040w	1056	1022	26.6
11	γ C–H	–	789	764	18.6
12	ν_{as} C–S, ν C–Cl	782s	776	751	421.6
13	ν_{as} C–S, ν C–Cl	730w	736	713	53.7
14	γ C–H, δ-ring	706w	712	689	42.2
15	ν_{as} C–S, ν C–Cl	505w	504	488	38.5
16	ν_{as} C–S, ν C–Cl	–	368	356	6.5
17	β C–S, γ C–Cl	–	248	240	34.1

[a] ν, stretching; ν_s, sym. stretching; ν_{as}, asym. stretching; β, in-plane-bending; γ, out-of-plane bending; δ, deformation.
[b] vs, very strong; s, strong; w, weak; ms, medium strong; m, medium.
[c] With the scale factor of 0.958 for calculated wave numbers greater than 3000 cm^{-1} and the scale factor of 0.9682 for lower wavenumbers.

asymmetric stretching and C–Cl stretching. This mode applies to the calculated frequency at 356 cm^{-1}. The theoretical frequency at 240 cm^{-1} is ascribed to the coupling of C–S in-plane bending and C–Cl out-of-plane bending, which is not observed in the experimental spectra.

Comparing the experimental IR spectra of the four title compounds with that of the parent compound DPS, we can see that there are no big changes in the C–H stretching vibrations since ν C–H of DPS occurs at 3073 cm^{-1} and 3058 cm^{-1}, and this vibration mode of the title compounds appear at 3081–3046 cm^{-1}. The C=C stretching vibrations of DPS are observed at 1580 cm^{-1}, 1476 cm^{-1} and 1439 cm^{-1}. However, when substituted with chlorine atoms, this vibration mode appears at 1562–1565 cm^{-1}, 1431–1434 cm^{-1} and 1397–1407 cm^{-1}. This phenomenon can be explained by the following words. For the title compounds, the negatively charged chlorine atoms (−0.05 to −0.01 e) make the electron density of the benzene ring reduced, leading to a decline in force constant of the C=C bond in the benzene ring. As a result, the C=C vibration frequencies shift to lower wave numbers.

4.3. NMR chemical shifts

The complete assignments of the peaks in the ^{1}H and ^{13}C NMR spectra are done by considering proton–proton couplings in experimental ^{1}H NMR spectra and C–H correlations in 2D experiment.

Table 6
Comparison of theoretical and experimental values of ^{1}H NMR chemical shifts.

Molecule	δ_H			Correlation analysis
	Cal.	Exp.	Assignments	
2,2′,3,3′-TCDPS	0.127	7.346	H-4 (H-4′)	$\delta_{H,exp} = -0.139 + 1.057\delta_{H,cal}$ $r^2 = 0.956$
	0.111	7.073	H-5 (H-5′)	
	0.126	6.968	H-6 (H-6′)	
2,2′,3,4′-TCDPS	0.146	7.528	H-3′	$\delta_{H,exp} = 4.842 + 0.344\delta_{H,cal}$ $r^2 = 0.957$
	0.123	7.349	H-4	
	0.107	7.092	H-5	
	0.129	7.254	H-5′	
	0.121	6.875	H-6	
	0.133	7.246	H-6′	
2,2′,3,5′-TCDPS	0.133	7.387	H-3′	$\delta_{H,exp} = 5.071 + 0.306\delta_{H,cal}$ $r^2 = 0.951$
	0.124	7.409	H-4	
	0.132	7.245	H-4′	
	0.107	7.133	H-5	
	0.121	6.862	H-6	
	0.145	7.161	H-6′	
2,2′,3,6′-TCDPS	0.129	7.501	H-3′ (H-5′)	$'5\delta_{H,exp} = 2.652 + 0.658\delta_{H,cal}$ $r^2 = 0.996$
	0.122	7.247	H-4	
	0.117	7.358	H-4′	
	0.106	6.984	H-5	
	0.120	6.408	H-6	

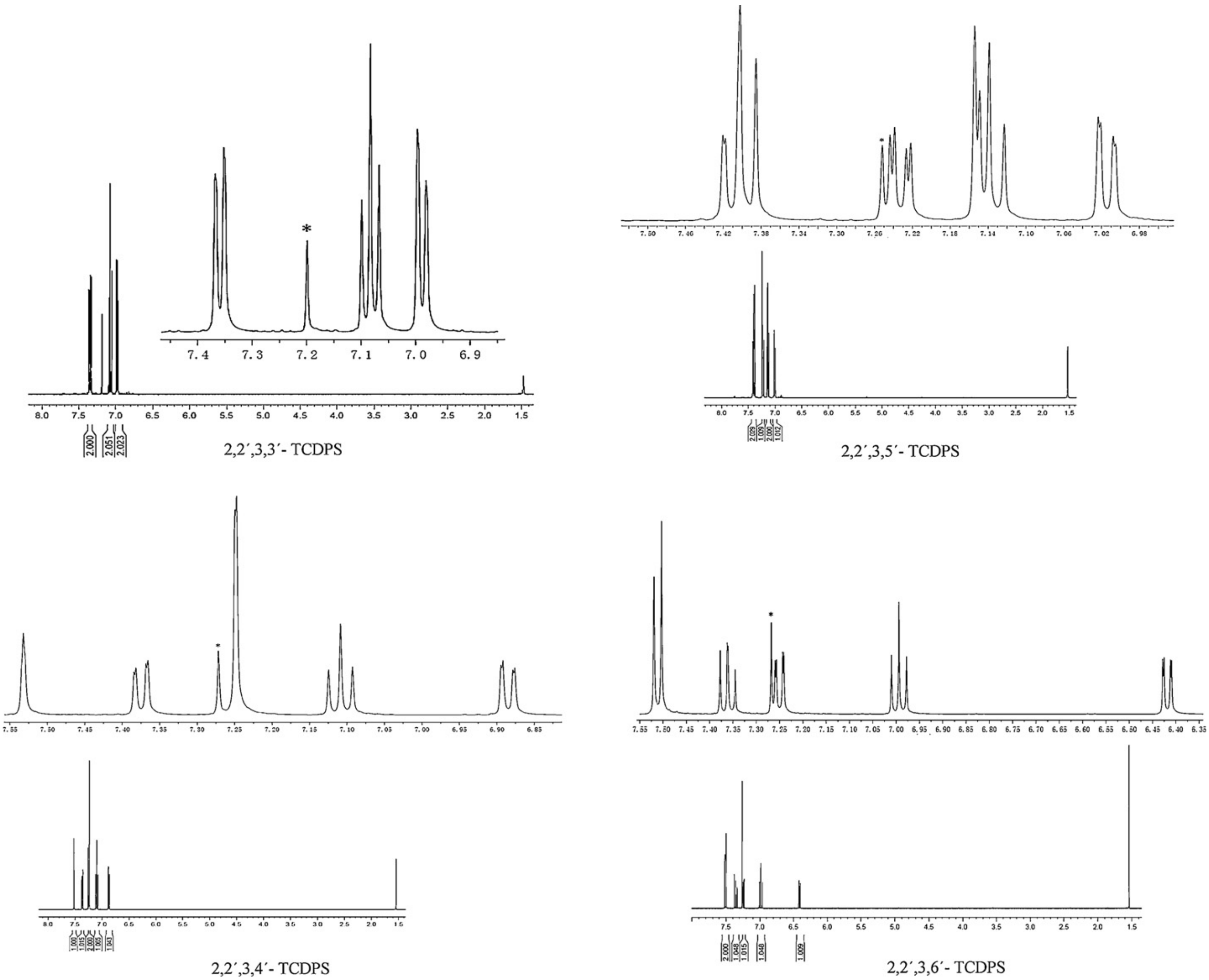

Fig. 3. Observed ^{1}H NMR spectrum of the 4 title compounds in $CDCl_3$ (The asterisk (*) indicates the peak of solvent $CDCl_3$).

The observed ^{1}H NMR spectra are denoted in Fig. 3. Table 6 lists theoretical chemical shifts of hydrogen atoms as well as relevant experimental values. In general, NMR signals of the protons on phenyl ring usually locate in the range of 6–8 ppm. Both calculated and experimental values of ^{1}H NMR chemical shifts are in the normal δ_H range. Furthermore, the correlation analyses of the theoretical and experimental data were carried out to check the goodness of fit. The results are also presented in Table 6. The squared correlation coefficients r^2 are all greater than 0.95. Therefore, these theoretical models may be used to predict the ^{1}H NMR chemical shifts.

Comparisons between ^{1}H NMR chemical shifts of the four title compounds and that of the parent compound DPS ($\delta_{H\text{-}2,6} = 7.204$, $\delta_{H\text{-}3,4} = 7.056$, $\delta_{H\text{-}5} = 7.004$ [32]) show that for the title compounds substituted with chlorine atoms, the chemical shifts of hydrogen atoms generally become larger (lower field). This is because the weakly electron-withdrawing chlorine atoms make the electric charge of hydrogen atoms on the benzene ring slightly decrease. However, the hydrogen at position 6 (6′) did not change significantly. Despite of the more positive charge H-6 carries, its chemical shift is smaller.

By analyzing the relationship between the chemical shift of hydrogen atom in the four title compounds and the electric charge it carries, the following conclusion can be drawn: except for the hydrogen at position 6 (6′), the hydrogen atom with larger positive charge (a smaller shielding effect) generally has a bigger chemical shift. For example, the charge of H-4 and H-5 in 2,2′,3,3′-TCDPS is 0.127 e and 0.111 e, respectively, and the corresponding chemical shift is 7.346 and 7.073. Although H-6 has more positive charge (0.126 e), its chemical shift is only 6.968.

With regard to carbon atoms, the calculated and measured chemical shifts are depicted in Table 7. The aromatic carbon in ^{13}C NMR spectra are expected to appear in the region of 110–135 ppm, and the experimental values of ^{13}C NMR chemical shifts are generally in the normal δ_C range. It can be seen clearly that the theoretical values show an excellent correlation with the experimental data, with r^2 going from 0.960 to 0.988.

In addition, the empirical values of ^{13}C chemical shift are also listed in Table 7. The results of Table 7 show that GIAO predictions are significantly better than the empirical ones for the title compounds due to the higher squared correlation coefficients.

Table 7
Comparison of theoretical and experimental values as well as empirical values of ^{13}C NMR chemical shifts.

Molecule	δ_C				Correlation analysis
	Cal.	Emp.	Exp.	Assignments	
2,2′,3,3′-TCDPS	150.572	137.6	135.293	C-1 (C-1′)	$\delta_{C,exp} = 83.648 + 0.344\delta_{C,cal}$
	146.327	136.7	134.124	C-2 (C-2′)	$r^2 = 0.988$
	145.127	134.8	133.522	C-3 (C-3′)	$\delta_{C,exp} = 45.725 + 0.648\ \delta_{C,emp}$
	132.531	128.8	129.711	C-4 (C-4′)	$r^2 = 0.796$
	135.598	128.6	130.425	C-5 (C-5′)	
	129.796	130.5	127.798	C-6 (C-6′)	
2,2′,3,4′-TCDPS	146.232	137.6	134.846	C-1	$\delta_{C,exp} = 80.959 + 0.365\delta_{C,cal}$
	129.916	136.7	129.010	C-2	$r^2 = 0.962$
	136.992	134.8	130.299	C-3	$\delta_{C,exp} = 67.555 + 0.484\delta_{C,emp}$
	131.283	128.8	128.602	C-4	$r^2 = 0.237$
	125.663	128.6	127.649	C-5	
	155.230	130.5	137.608	C-6	
	139.108	134.3	130.537	C-1′	
	150.274	137.2	136.238	C-2′	
	134.837	129.9	128.892	C-3′	
	149.554	133.7	135.203	C-4′	
	129.247	127.4	128.125	C-5′	
	143.939	133.8	133.968	C-6′	
2,2′,3,5′-TCDPS	146.325	137.6	134.147	C-1	$\delta_{C,exp} = 93.345 + 0.278\delta_{C,cal}$
	145.489	136.7	134.065	C-2	$r^2 = 0.960$
	143.584	134.8	133.328	C-3	$\delta_{C,exp} = 67.136 + 0.489\delta_{C,emp}$
	130.130	128.8	129.673	C-4	$r^2 = 0.483$
	139.356	128.6	132.182	C-5	
	125.929	130.5	127.820	C-6	
	140.376	137.6	133.216	C-1′	
	152.417	134.4	135.084	C-2′	
	135.131	130.9	131.169	C-3′	
	129.351	128.8	129.249	C-4′	
	149.423	132.5	134.422	C-5′	
	135.113	132.8	130.046	C-6′	
2,2′,3,6′-TCDPS	148.856	137.6	137.563	C-1	$\delta_{C,exp} = 59.892 + 0.516\delta_{C,cal}$
	134.316	136.7	129.197	C-2	$r^2 = 0.968$
	146.156	134.8	133.573	C-3	$\delta_{C,exp} = 17.297 + 0.857\delta_{C,emp}$
	129.606	128.8	127.463	C-4	$r^2 = 0.440$
	129.196	128.6	127.083	C-5	
	124.513	130.5	124.017	C-6	
	137.868	136.6	129.539	C-1′	
	157.599	137.7	142.140	C-2′ (C-6′)	
	132.515	127.6	129.078	C-3′ (C-5′)	
	139.180	129.8	131.631	C-4′	
Overall					$\delta_{C,exp} = 75.235 + 0.405\delta_{C,cal}$
					$r^2 = 0.938$
					$\delta_{C,exp} = 48.599 + 0.626\delta_{C,emp}$
					$r^2 = 0.388$

5. Conclusion

IR and NMR spectra of 4 synthesized TCDPSs were studied by means of theoretical calculation and experiment. The harmonic vibration frequencies in IR, ^{1}H NMR and ^{13}C NMR chemical shifts of the title compounds were calculated at the B3LYP/6-311G** level by using the Gaussian 03 program. The scaled theoretical vibration frequencies show good accordance with the experimental values. The chemical shifts of both hydrogen and carbon atoms agree well with the observations. The higher correlation coefficients ($r^2 > 0.93$) of the obtained regression equations indicate that the calculated chemical shifts may reproduce the experimental data.

Acknowledgement

This work was financially supported by the National Natural Science Foundation of China (41071319, 20977046, 20737001).

Appendix A. Supplementary data

Supplementary data associated with this article can be found, in the online version, at doi:10.1016/j.saa.2011.06.008.

References

[1] T. Nevalainen, E. Kolehmainen, K. Rissanen, M.L. Stiffmen, R. Kauppinen, Magn. Reson. Chem. 31 (1993) 100–104.

[2] A. Mostrag, T. Puzyn, M. Haranczyk, Environ. Sci. Pollut. R 17 (2010) 470–477.

[3] M. Abalos, X. Prieto, J.M. Bayona, J. Chromatogr. A 963 (2002) 249–257.

[4] J.T. Anderson, S. Bobinger, Chemosphere 24 (1992) 383–389.

[5] S. Sinkkonen, E. Kolehmainen, K. Laihia, J. Koistinen, T. Rantio, Environ. Sci. Technol. 27 (1993) 1319–1326.

[6] V.A. Zubkov, T.M. Birshtein, I.S. Milevskaya, J. Mol. Struct. 27 (1975) 139–149.

[7] M.H. Habibi, H. Vosooghian, J. Photochem. Photobiol. A: Chem. 174 (2005) 45–52.

[8] I.P. Nnane, L.A. Damani, J. Pharm. Biomed. Anal. 27 (2002) 315–325.

[9] T. Sumiyoshi, H. Sakai, M. Kawasaki, M. Katayama, Chem. Lett. 21 (1992) 617–620.

[10] H.W. Zhu, J.L. Jiang, Z.Y. Wang, L.S. Wang, H.X. Yu, Acta Chim. Sinica 66 (2008) 1139–1150.

[11] D.B. Chesnut, Annu. Rep. NMR Spectrosc. 21 (1989) 51–97.

[12] D.B. Chesnut, Annu. Rep. NMR Spectrosc. 29 (1994) 71–122.

[13] V. Barone, R. Improta, N. Rega, Acc. Chem. Res. 41 (2008) 605–616.

[14] K. Wolinski, J.F. Hilton, P. Pulay, J. Am. Chem. Soc. 112 (1990) 8251–8260.

[15] A. Bax, R.H. Griffey, B.L. Hawkins, J. Magn. Reson. 55 (1983) 301–315.

[16] R. Ditchfield, Mol. Phys. 27 (1974) 789–807.

[17] R.J. Abraham, G.H. Grant, I.S. Haworth, P.E. Smith, J. Comput. Aided Mater. Des. 5 (1991) 21–39.

[18] S.S. Qiu, X.H. Tan, K. Wu, A.Q. Zhang, S.K. Han, L.S. Wang, Spectrochim. Acta A 76 (2010) 429–434.

[19] M.J. Frisch, G.W. Trucks, H.B. Schlegel, G.E. Scuseria, M.A. Robb, J.R. Cheeseman, J....A. Montgomery Jr., T. Vreven, K.N. Kudin, J.C. Burant, J.M. Millam, S.S. Iyengar, J. Tomasi, V. Barone, B. Mennucci, M. Cossi, G. Scalmani, N. Rega, G.A. Petersson, H. Nakatsuji, M. Hada, M. Ehara, K. Toyota, R. Fukuda, J. Hasegawa, M. Ishida, T. Nakajima, Y. Honda, O. Kitao, H. Nakai, M. Klene, X. Li, J.E. Knox, H.P. Hratchian, J.B. Cross, V. Bakken, C. Adamo, J. Jaramillo, R. Gomperts, R.E. Stratmann, O. Yazyev, A.J. Austin, R. Cammi, C. Pomelli, J.W. Ochterski, P.Y. Ayala, K. Morokuma, G.A. Voth, P. Salvator, J.J. Dannenberg, V.G. Zakrzewski, S. Dapprich, A.D. Daniels, M.C. Strain, O. Farkas, D.K. Malick, A.D. Rabuck, K. Raghavachari, J.B. Foresman, J.V. Ortiz, Q. Cui, A.G. Baboul, S. Clifford, J. Ciomslowski, B.B. Stefanov, G. Liu, A. Liashenko, P. Piskorz, I. Komaromi, R.L. Martin, D.J. Fox, T. Keith, M.A. Al-Laham, C.Y. Peng, A. Nanayakkara, M. Challacombe, P.M.W. Gill, B. Johnson, W. Chen, M.W. Wong, C. Gonzalez, J.A. Pople, Gaussian 03, D. 01, Gaussian Inc., Wallingford, CT, 2004.

[20] R. Dennington II, T. Keith, J. Millam, GaussView, Version 4. 1, Semichem Inc., Shawnee Mission, KS, 2007.

[21] X.S. Zhang, L. Sun, J.Q. Shi, Z.Y. Wang, Chinese J. Org. Chem. 31 (2011) 1189–1195.

[22] B. Rozsondai, J.H. Moore, D.C. Gregory, I. Hargittai, Acta. Chim. Acad. Sci. Hung 94 (1977) 321–331.

[23] Y. Ye, M. Ruan, Y.Z. Song, Y.Y. Li, W. Xie, Spectrochim. Acta A 68 (2007) 85–93.

[24] P.M. Wojciechowski, D. Michalska, Spectrochim. Acta A 68 (2007) 948–955.

[25] D. Michalska, W. Zierkiewicz, D.C. Bienko, W. Wojciechowski, J. Phys. Chem. A 105 (2001) 8734–8739.

[26] J.P. Merrick, D. Moran, L. Radom, J. Phys. Chem. A 111 (2007) 11683–11700.

[27] V. Krishnakumar, R. John Xavier, Indian J. Pure Appl. Phys. 41 (2003) 597–601.

[28] N. Sundaraganesan, B. Anand, C. Meganathan, B.D. Joshua, Spectrochim. Acta A 69 (2008) 871–879.

[29] G. Socrates, Infrared and Raman Characteristic Group Frequencies—Tables and Charts, third ed., Wiley, New York, 2001.

[30] E.F. Mooney, Spectrochim. Acta 19 (1963) 877–887.

[31] E.F. Mooney, Spectrochim. Acta 20 (1964) 1021–1032.

[32] K. Hayamizu, O. Yamamoto, J. Mol. Spectrosc. 25 (1968) 422–435.